聚丙烯腈基炭纤维对比分析:(二)结构与性能的关联性

郝俊杰[1], 吕春祥[2], 李登华[3]
(1. 山西钢科碳材料有限公司,山西 太原 030100;
2. 中国科学院山西煤炭化学研究所 碳纤维制备技术国家工程实验室,山西 太原 030001;
3. 山西省交通科技研发有限公司 新型道路材料国家地方联合工程实验室,山西 太原 030032)

摘 要: 以典型聚丙烯腈基炭纤维为研究对象,结合弹性解皱模型、Griffith微裂纹理论等探讨了炭纤维的力学性能与微观结构的关联性。分别分析了微晶结构及其择优取向对拉伸模量、孔结构及质量密度起伏对拉伸强度、内部残余压缩应力对断裂伸长率的影响关系,确认了上述对炭纤维力学性能起关键影响作用的结构因素,并据此探讨了炭纤维的拉伸断裂机制。

关键词: 炭纤维;晶态结构;力学性能;结构不均匀性;分形
中图分类号: TQ324$^+$.74 **文献标识码:** A

基金项目:山西省重点研发计划项目(201903D121005);山西省科技重大专项(20181101019).
通讯作者:李登华,博士,高级工程师. E-mail: yob2846@163.com
作者简介:郝俊杰,博士,工程师. E-mail: haojj@tisco.com.cn

A comparative analysis of polyacrylonitrile-based carbon fibers: (Ⅱ) Relationship between the microstructures and properties

HAO Jun-jie[1], LU Chun-xiang[2], LI Deng-hua[3]
(1. *Shanxi Gangke Carbon materials Co., Ltd, Taiyuan* 030100, *China*;
2. *National Engineering Laboratory for Carbon Fiber Technology, Institute of Coal Chemistry, Chinese Academy of Sciences, Taiyuan* 030001, *China*;
3. *National and Local Joint Engineering Laboratory of Advanced Road Materials, Shanxi Transportation Technology Research & Development Co., Ltd, Taiyuan* 030032, *China*)

Abstract: The relationships between the mechanical properties and the microstructures of typical polyacrylonitrile-based carbon fibers were studied on the basis of the elastic wrinkle model and Griffith microcrack theory. The effects of microcrystallite structure and its preferred orientation on tensile modulus, the effects of microvoids and mass density changes on the tensile strength, and the effects of internal residual compressive stress on the strain to failure, were analyzed, based on which the structural factors played a key role in determining the mechanical properties of the fibers.

Key words: Carbon fiber; Crystalline structure; Mechanical property; Structural heterogeneity; Fractal

Received date: 2020-03-26; *Revised date*: 2020-07-01
Foundation item: Key Research and Development (R&D) Projects of Shanxi Province (201903D121005); Science and Technology Major Project of Shanxi Province (20181101019).
Corresponding author: LI Deng-hua, Ph. D, Senior engineer. E-mail: yob2846@163.com
Author introduction: HAO Jun-jie, Ph. D, Engineer. E-mail: haojj@tisco.com.cn

1 Introduction

As a novel reinforcing material, carbon fiber has a range of outstanding properties such as high specific strength, high specific modulus, high electrical conductivity, high thermal conductivity, low density and heat resistance. Moreover, as a fiber, it also possesses flexibility, self-lubricity, and can be knitted and woven, which has thus gained broad applications in the cutting-edge fields like aerospace, defense technology, as well as the civilian fields like high-end sporting goods and medical equipment[1-5]. According to literature, the mechanical properties of carbon fibers are determined primarily by the structural defects inside them or on their surface[6]. The majority of these defects are inherited from the precursor fibers, which exist in the forms of micropores, surface defects, etc. Their structural morphology, size and distribution are linked closely to the process control accuracy during the fabrication process[7,8]. With the

advancement of carbon fiber fabrication process and process control technology in recent years, a variety of carbon fiber products with differing performances have been introduced to the market successively, which have become a prominent reinforcing material among composites[5]. For these high-performance fibers, the structural stability and refinement have growingly become their common characteristics[9]. Today, it is difficult to detect the defects on the surface or inside of a typical commercial carbon fiber simply by intuitive means such as electron microscopy. In other words, the high-precision carbon fiber fabrication process and process control technology have helped eliminate the existence of large-size defects greatly[10]. From another aspect, the high performance of carbon fiber is achieved by precise control of the fine structure and large-scale defects. In this context, carbon fibers with large-size defects have been wiped out. Then, what are the roots or constraints for their mechanical properties?

From the comparison of mechanical properties among typical commercial carbon fibers, it is not difficult to find that aside from having high tensile strength, the elongation at break of high-strength carbon fibers is also at a high level generally. Given the high elongation at break, the modulus of such type of fibers is rather low. High-modulus carbon fibers, on the other hand, generally have a low elongation at break, and accordingly their modulus increases rapidly. As this study finds, the differences in mechanical properties between the above two types of fibers are correlated with their microstructure discrepancies and the resulting differences in their fracture mechanisms. Besides, the differences in mechanical properties can also be explained by the diversity of microstructures. On this basis, after systematic comparative analysis of the crystalline structure, pore structure, radial structure heterogeneity, graphitization degree, internal residual stress, structural orientation and fractal phenomenon for different types of carbon fibers, this study explores the correlation between the mechanical properties and microstructures of carbon fiber by employing the elastic wrinkle model and Griffith microcrack theory. Findings of this study are expected to provide a support and theoretical guidance for the research and stable production of high-performance carbon fibers in China.

2 Experimental

2.1 Specimens

The present experiment was conducted using various polyacrylonitrile (PAN)-based carbon fibers, all of which were purchased from Toray Industries. Their basic information is shown in Table 1:

Table 1　Properties of carbon fibers from Toray Industries, Inc[6].

Product No.		Filaments	Tensile strength /GPa	Tensile modulus /GPa	Elongation at break /%	Density /g cm^{-3}
T series	T300B	6K	3.53	230	1.5	1.76
	T700SC	12K	4.90	230	2.1	1.80
	T800H	6K	5.49	294	1.9	1.81
	T1000G	12K	6.37	294	2.2	1.80
MJ series	M40JB	6K	4.41	377	1.2	1.77
	M55JB	6K	4.02	540	0.8	1.91
	M60JB	6K	3.92	588	0.7	1.93

2.2 Structural characterization

An AG-1 universal testing machine (Shimadzu Co., Ltd., Japan) was utilized to test the mechanical properties of various types of carbon fibers in accordance with the GB/T 3362-2017 Test Methods for Tensile Properties of Carbon Fiber Multifilament. The density of the carbon fibers was measured in a density gradient column in accordance with the GB/T 30019-2013 Measurement of Carbon Fiber Density. Raman spectroscopy tests were performed on a XPLORA and LabRam HR Evolution Raman spectrometers (Jobin-Yvon, Horiba).

Wide-angle X-ray diffraction (WAXD) was performed on a PANalytical X'Pert PRO X-ray diffractometer (Cu Kα, λ = 0.154 1 nm, 40 kV, 40 mA). The diffraction curves were fitted by the MDI Jade 5.0, and the structure parameters of all samples were obtained as follows. The (002) peak from the equatorial scan was used to estimate the value of the average interlayer spacing, $d_{(002)}$, which was calculated based on the Bragg's law[6]:

$$d_{(002)} = \frac{\lambda}{2\mathrm{Sin}\theta} \tag{1}$$

Where λ is the wavelength of the X-ray, and θ is the scattering angle. The (002) peak from the equatorial scan was also used to calculate the apparent crystallite stacking thickness, L_c. Meanwhile, the apparent dimensions of crystallites parallel and perpen-

dicular to the fiber axis, $L_{a//}$ and $L_{a\perp}$ were estimated by using the meridian scan and equatorial scan of the (100) peak, respectively. All the crystallite sizes, L_c and L_a were calculated using the Scherrer's formula[6]:

$$L = \frac{K\lambda}{\beta\cos\theta} \quad (2)$$

Where β is the full width at half maximum intensity (FWHM), and the form factor K is 0.89 for L_c and 1.84 for L_a[6].

Small-angle X-ray scattering (SAXS) experiments were performed on a SAXSess mc2 SAXS system (Anton Paar Co., Ltd., Austria). Approximately 1 mm thick bundles of fibers were arranged parallel on the sample holder to conduct the experiment. The scattered X-ray intensity was recorded using an image plate detector, and each measurement was recorded for 1 h. The desmearing of collimating error and the background correction of SAXS data were done by the SAXS-quant 1.01 software included with the instrument[11-14]. For the determination of parameters from SAXS several options were available, namely Porod, Guinier and Debye-Bueche methods. They were generally well-established and applicable for the quasi two-phase system of carbon fibers as suggested in many related articles[1, 2]. Based on the Porod's law the influence of the local density fluctuation on the structural analysis could be examined[11-13]:

$$I_{obs}(q) = I(q) + I_{fl}(q) = \frac{K}{q^4}\exp(bq^2) \quad (3)$$

Where $I_{obs}(q)$ is the observed SAXS intensity using a pinhole collimating system, $I(q)$ is the intensity component followed the Porod's law, $I_{fl}(q)$ is a constant modelling the scattered intensity from electron density fluctuation in the phases, b is the Porod factor which represents the deviation from a typical two-phase system in this study, and the scattering vector is calculated by $q = 4\pi\sin\theta/\lambda$. Based on the Debye-Bueche method, the intensity component caused by microvoids could be separated from the total intensity and thus the radial dimension of microvoids could be determined by[11,12]:

$$l_x = 2\frac{\int_0^\infty qI(q)\,dq}{\int_0^\infty q^2 I(q)\,dq} \quad (4)$$

In a certain fractal system, the scattering intensity $I(q)$ corresponding to each q follows[13,14]:

$$\ln I(q) = \ln I_0 - \alpha \ln q \quad (5)$$

where I_0 is a constant, α is a parameter related to the fractal dimension ($0 < \alpha < 4$). Surface fractal can be determined if the $\ln I(q) \sim \ln q$ curve returned $3 < \alpha < 4$, and here the fractal dimension is given by[13,14]:

$$D_s = 6 - \alpha \quad (6)$$

Where D_s is the surface fractal dimension which to some extent represents the roughness of the internal surface.

3 Results and discussion

3.1 Effects of the crystallite structure on tensile modulus

It is universally acknowledged that the tensile modulus of carbon fibers is affected directly by their crystallite structure[6]. In this paper, a combination of WAXD and Raman spectroscopy was used to analyze the correlation between microstructure parameters and tensile modulus of carbon fibers. In Fig. 1, the tensile modulus variations of carbon fibers with crystallite parameters are illustrated. It is clear that the tensile modulus exhibits significant correlations with the orientation angle z and the interlayer spacing d_{002} of crystallites. As the interlayer spacing and orientation angle increase, the tensile modulus of carbon fibers tends to decrease gradually. Such trends approximate linear relationships.

Similarly, with the increase of crystallite dimensions (stack thickness L_c, in-plane size L_a), both types of carbon fibers exhibit significant increases in tensile modulus, and such an increasing trend is not directly related to the category of fiber series. This phenomenon has been verified with both the reflection and transmission mode of WAXD. Agreeing well with the previous conclusion, the modulus may be simply a mechanical parameter that is related to the degree of perfection of fibers´crystalline structure, including crystallite dimensions, interlayer spacing, preferred orientation, etc.

Aside from the crystalline data obtained by WAXD, other parameters like graphitization degree derived from Raman spectroscopy are also correlated to the tensile modulus of carbon fibers. In Fig. 2, the correlation between the graphitization degree A_D/A_G and the tensile modulus is depicted for carbon fibers. As the data demonstrates, the graphitization degree, which is closely related to the fiber crystallite structure, presents a similar pattern of effect on the tensile modulus as the crystallite structure does. With increasing the degree of graphitization, the tensile modulus decreases in a nearly linear manner, suggesting that the enhancement of graphitization is conducive to attaining high modulus. Additionally, the graphitization degrees of fiber sheath and core have the similar effects on the tensile strength and modulus. This suggests that despite varying degrees of the radial structure heterogeneity among the carbon fibers, their impact on tensile modulus is insignificant.

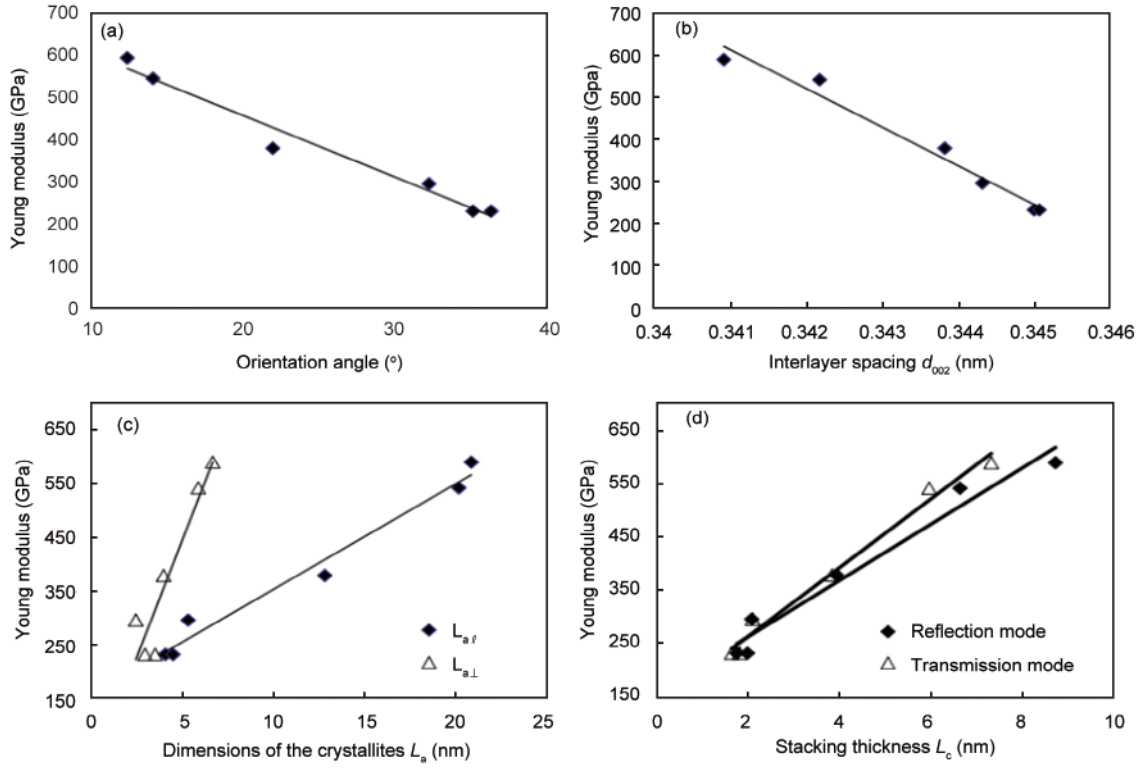

Fig. 1　The dependence of Young modulus on (a) orientation angle, (b) interlayer spacing, (c) dimensions of crystallites and (d) stacking thickness.

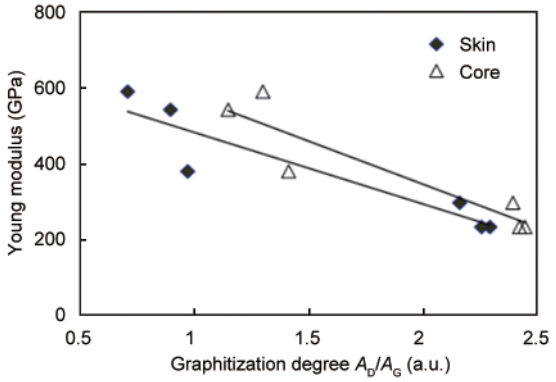

Fig. 2　The dependence of Young modulus on the graphitization degree of the core and the skin of carbon fibers.

Similar to the effects of the crystalline structure on the tensile strength and elongation at break, the above data all indicate that the tensile modulus of carbon fibers is correlated directly with the degree of their crystalline structure perfection. To obtain a high-modulus carbon fiber, the only way is to improve its crystallite structure parameters and perfect the ordered stacking of its disorderly graphite structure.

3.2　Effects of the microstructure on tensile strength

The Griffith microcrack theory, as the foundation of fracture mechanics for brittle materials, links defects such as cracks in brittle materials to the tensile strength[6]. For carbon fibers, which are a kind of brittle materials, structural defects are also a fundamental factor affecting their tensile strength. The Griffith microcrack theory is expressed as follows[15]:

$$\sigma = \sqrt{\frac{2E_C\gamma_F}{\pi C}} \tag{7}$$

Where σ denotes the tensile strength (Pa), C denotes the size of structural defect (m), E_C denotes the tensile modulus of carbon crystallites and γ_F is the free surface energy of fracture (J m^{-2}). From the above equation, it is clear that the tensile strength of carbon fibers is linearly correlated with the reciprocal square root of the defect size, and the data herein supports this point[16].

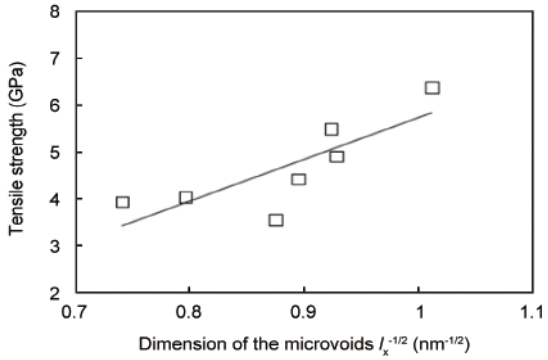

Fig. 3　The dependence of tensile strength on the radial dimension of microvoids $l_X^{-1/2}$.

Owing to the advancement of fabrication process, the large-size cracks, pores and defects in high-performance carbon fibers have been eliminated fundamentally. Hence, the internal defects that constitute the fracture origin of carbon fibers are mostly the internal nano-scale voids. In Fig. 3, the linear relationship between the tensile strength of various types of carbon fibers and the reciprocal square root of the radial size of their internal pores is depicted. It can be confirmed from the figure that the pore defects have a direct impact on the tensile strength. However, the functional relationship between the two is a straight line with a slope and intercept, rather than a straight line that passes through the origin (0,0). Obviously, there are factors other than the voids affects the tensile fracture process of carbon fibers, either directly or indirectly.

Correlations are found regarding both the Porod coefficient and surface fractal dimension in the SAXS analyses with the tensile strength. As shown in Fig. 4, with the increase in these two parameters, the tensile strength of carbon fibers presents a nonlinear growth. The Porod coefficient characterizes the fluctuation of mass density at the carbon fiber microdomains. And the surface fractal dimension is a measure of the complexity of the microdomain structure, both of which may exert an impact on the tensile strength by affecting the free surface energy of fracture[17,18]. This implies that for carbon fibers, the stronger the microstructure fluctuations in mass density and the higher the complexity of fracture surface, the more work needs to be applied for achieving tensile fracture. All in all, reducing the number of micro-defects and the size of micro-pores and enhancing the complexity of microstructures all contribute to the improvement of carbon fiber strength.

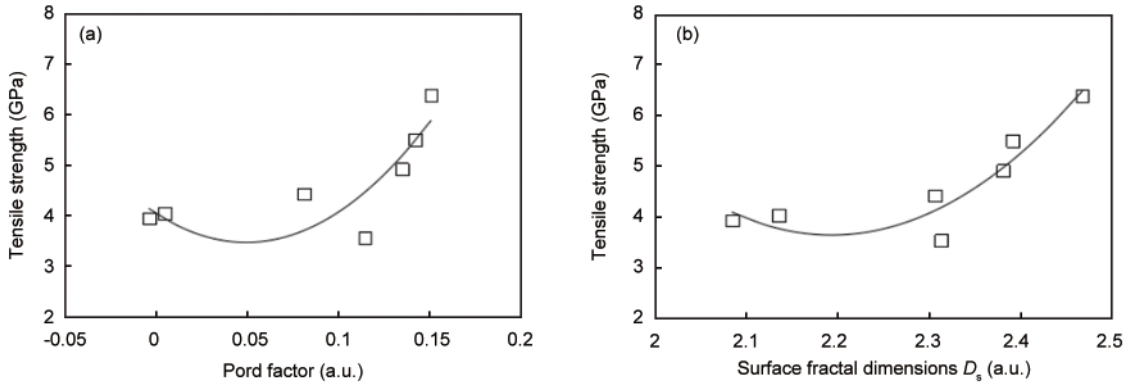

Fig. 4 The dependence of tensile strength on (a) Porod factor and (b) surface fractal.

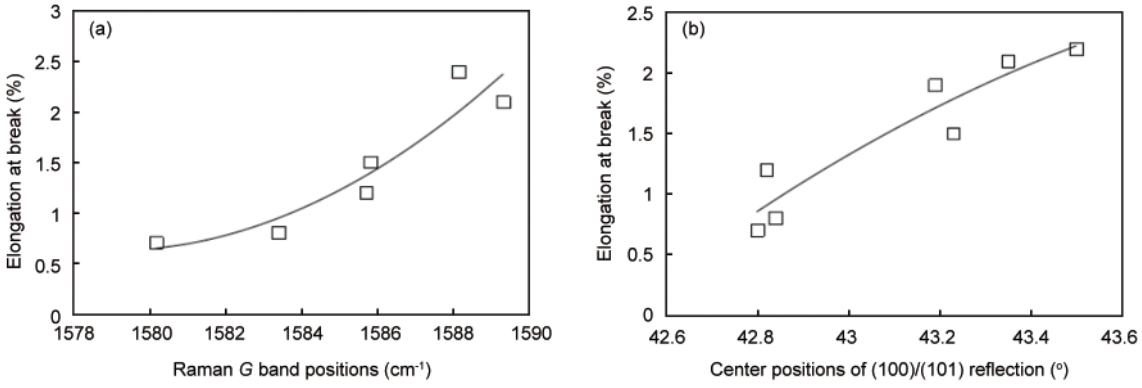

Fig. 5 The dependence of elongation at break on (a) Raman *G* band shifts and (b) positions of (100)/(101) reflection.

3.3 Effects of the microstructure on elongation at break

Elongation at break is an indicator that is easily overlooked in the research of carbon fiber mechanical properties. In fact, it is a very important indicator, which characterizes the deformability of carbon fibers under tensile stress, and interacts with the tensile strength and modulus. A significant correlation is found between the elongation at break and the micro-residual stress existing inside the carbon fibers. In Fig. 5, the effects of Raman *G* peak shift and (100)/(101) peak position on the elongation at break of carbon fibers are illustrated. As the data demonstrates, with the shift of *G* peak towards a high wavenumber or the shift of (100)/(101) peak towards a high angle, the elongation at break presents a gradual upward trend.

In our prior research, it is found by our group hat the differences in Raman *G* peak shift and (100)/(101)

peak position among various types of carbon fibers should be attributed to the varying levels of compressive residual stress inside. Such compressive stress was released in a slow, gradual manner under the temperature and stress fields, which further led to the *G* peak shift towards a low wavenumber and the (100)/(101) peak shift towards a low angle region. The limit of such compressive stress during natural release is the ideal state of standard graphite. In other words, under the action of temperature and stress fields, the limit of *G* peak shifts towards a low wave number at ~1 580 cm^{-1}, namely the E_{2g2} vibration mode of ideal graphite, while the limit of (100)/(101) peak shift towards a low angle region reaches ~0.213 5 nm, namely the 100 plane layer spacing of ideal graphite[19]. At that point, the compressive stress inside carbon fibers is released sufficiently, the curled and contracted state of graphite-like structure is eliminated completely, and the C—C bond length is close to the reported value for an ideal graphite, i.e. 0.142 1 nm.

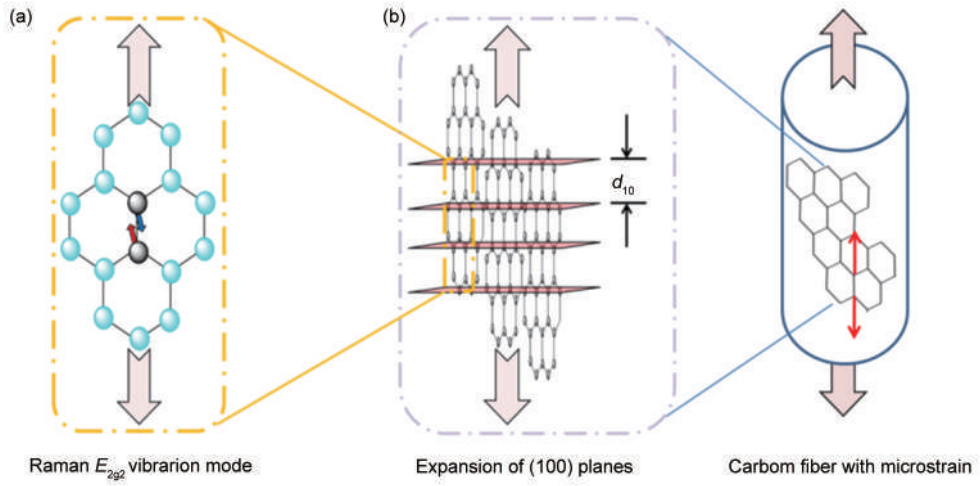

Fig. 6　Schematic diagrams of (a) in-plane E_{2g2} vibration mode in Raman spectroscopy and (b) the expansion of (100) planes along the fiber axis according to WAXD [13].

Fig. 6 shows the schematics of Raman E_{2g2} vibration mode and 100 plane elongation along the fiber axis in WAXD under tensile stress. Both methods of characterization reflect the stress/strain changes along the fiber axis in the graphite-net plane. The *G* peak shift and (100)/(101) peak position are used as the measures of residual compressive stress/strain state for the carbon fibers. Their correlations with the elongation at break suggest that the strain of carbon fibers under tensile stress is precisely a process in which the internal compressive stress/strain undergoes deformation in response to the external stress. This constitutes an important part of the tensile fracture mechanism for the carbon fibers.

3.4　Discussion on the tensile fracture mechanism of carbon fibers

Although the above results explain the microstructural factors that are critically influential to the tensile strength, elastic modulus and elongation at break of carbon fibers, a comprehensive and deeper probe into the correlation between the microstructure and tensile fracture mechanism are still needed, in order to understand the tensile fracture mechanism of the fibers. In prior studies, we analyzed the correlation between the tensile modulus of carbon fibers and their structural characteristics by using the elastic wrinkle model as the theoretical basis, and found that the model used conformed basically to the laboratory data and production parameters, which was capable of explaining many experimental phenomena in this paper as well[20-22].

The relationship between tensile modulus and the preferred orientation parameters is expressed by the following formula[20, 21]:

$$\frac{1}{E_c} = l_z S_{11} + k m_z \tag{8}$$

Where E_c denotes the tensile modulus that is corrected with the following formula:

$$E_c = E_{obs}\frac{\rho_c}{\rho_{obs}} \tag{9}$$

In the formula, ρ_{obs} denotes the apparent bulk density of carbon fiber, E_{obs} denotes the apparent tensile modulus and ρ_c is the crystal density determined according to d_{10} and d_{002}, whose value can be derived with the method recommended by Northolt et al[19]. Meanwhile, S_{11} denotes the in-plane flexibility of hexagonal carbon network, k denotes the environmental resistance against the tilting of plane, and l_Z, m_Z are the weighted means of function $g(\varphi)$, both of which are functions that characterize the preferred orientation degree of carbon crystallites. The elastic wrinkle model

emphasizes the contribution of the mechanical strength of carbon hexagonal plane to the macro-mechanical properties, which associates the macro-elastic modulus to the mechanical properties and preferred orientation characteristics of the carbon hexagonal plane. So it is not hard to understand the presence of a direct correlation between the tensile modulus of carbon fibers and the preferred orientation angle z of their crystalline structure. Noteworthy is that during the fabrication of carbon fibers, with the application of high-temperature and drawing tension, the crystallite orientation rearrangement and the internal compressive stress release occur synchronously, and the crystalline structure orientation optimization and the full-dimensional crystallite growth occur simultaneously as well[23,24]. The well-crystallized carbon fiber crystallites also have a high degree of preferred orientation in general, which gives rise to the phenomenon of associations of crystallite stack thickness L_c, in-plane size L_a, interlayer spacing d_{002} and orientation angle z with the tensile modulus[25], as shown in Fig. 1. What needs to be clarified here is that according to the elastic wrinkle model, the preferred orientation of the crystalline structure is the primary influencing factor of elastic modulus, while the remaining crystalline structure parameters may be in a subordinate position only[20].

The aforementioned contents of internal compressive stress form a supplement to the theory of elastic crease removal. The elastic crease removal is precisely a process in which the internal compressive stress is forced to be released, the crystallites are restructured and rearranged, and the carbon fiber is elongated and strained axially. Here, the correlations of elongation at break with the Raman G peak shift and the (100/101) peak position are also incorporated into the theory of elastic crease removal, thereby summarizing the tensile fracture mechanism of carbon fibers as follows:

(1) As shown in Fig. 7, the tensile fracture of high-strength carbon fibers needs to undergo at least three key stages, which, starting from the application of stress, are the release process of internal stress, the process of fracture origin formation and crack propagation and the final process of fracture failure, successively.

(2) After the application of external stress, the internal residual compressive stress is forced to be decompressed. At this point, with the gradual release of residual stress, the Raman G peak shifts towards a low wavenumber, while the (100)/(101) peak position shifts towards a low angle direction[26]. Of particular noteworthy mention is that the release process of internal stress is also a process of internal crystallite orientation fine-tuning and the elastic crease removal of curled carbon layers. This is also why some researchers have found the enhancement of preferred orientation resulting from the optimization of the crystalline structure upon application of tensile stress[26,27].

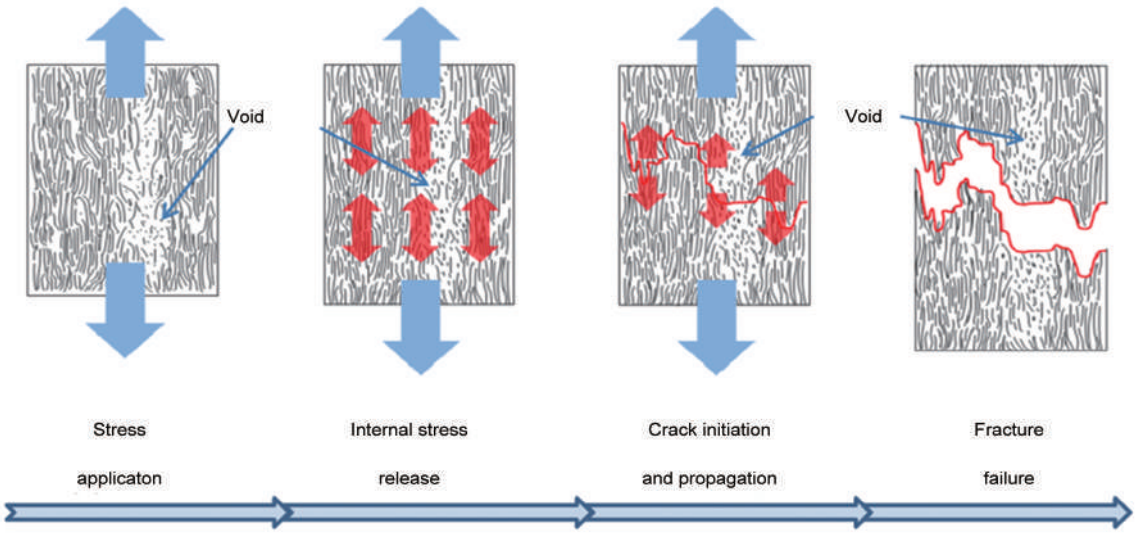

Fig. 7 Tensile fracture mechanism of carbon fibers[22].

(3) The state of internal residual stress (with reference to the initial positions of Raman G peak and (100)/(101) peak) determines the tensile elongation limit of carbon fibers, while the mechanical properties of the crystallite carbon hexagonal plane and its degree of orientation (with reference to the preferred orientation angle z of the crystalline structure) determines the limit of tensile elastic modulus.

(4) The occurrence of fracture origin depends on the size and quantity of internal porous structure (with a reference to the radial pore size and porosity derived by SAXS), whereas the propagation of cracks is influenced by parameters related to free surface energy of fracture, such as the mass density fluctuation at the microdomains (with a reference to the Porod coefficient derived by SAXS) and the surface complexity (with a reference to the surface fractal dimension derived by SAXS). The fracture origin and its propagation process together determine when the tensile fracture occurs, i. e. determine the tensile strength of carbon fibers.

(5) No significant differences are noted in the tensile fracture mechanism between the high-strength T series and the high-modulus MJ series fibers. Nevertheless, the MJ series present enhanced preferred orientation due to their smaller internal compressive stress (both the *G* peak and (100)/(101) peak positions of the MJ series are lower than those of the T series), more intact crystalline structure and milder curled state of crystallites. Therefore, they feature higher tensile elastic modulus of carbon fibers. Meanwhile, it is also precisely because of the smaller internal residual stress that the internal stress release/elastic crease removal process of this series is significantly shorter than the T series. As a result, the elongation at break of MJ series is significantly lower than the T series.

4 Conclusions

In this paper, the correlations between mechanical properties and microstructures of carbon fibers are explored based on the elastic wrinkle model and Griffith microcrack theory. The effects of crystallite structure and its preferred orientation on tensile modulus, of microvoids and mass density fluctuation on tensile strength, and of residual compressive stress on elongation at break are analyzed. Accordingly, the structural factors which have played a critical role in the mechanical properties of the fibers are identified, based on which the tensile fracture mechanism is proposed and discussed.

References

[1] Ruland W. Carbon fibers [J]. Advanced Materials, 1990, 2 (11): 528-536.

[2] Jahromi S G, Khodaii A. Carbon fiber reinforced asphalt concrete [J]. Arabian Journal Forence & Engineering, 2008, 33 (2): 355-564.

[3] Böhm R, Thieme M, Wohlfahrt D, et al. Reinforcement systems for carbon concrete composites based on low-cost carbon fibers [J]. Fibers, 2018, 6(3): 56.

[4] Hou X, Cheng W, Chen N, et al. Preparation of a high performance carbon/carbon composite throat insert woven with axial carbon rods [J]. New Carbon Materials, 2013, 28(5): 355-362.

[5] Yang Y H, Pan Y X, Feng Z H, et al. Evaluation of aerospace carbon fibers[J]. New Carbon Materials, 2014, 29(3): 161-168.

[6] He F. Carbon Fibre and Graphite fibre[M]. Beijing: Chemical Industry Press, 2010.

[7] Kobets L, Deev I. Carbon fibres: Structure and mechanical properties [J]. Composites Science and Technology, 1998, 57 (12): 1571-80.

[8] Guigon M, Oberlin A. Heat-treatment of high tensile strength PAN-based carbon fibres: Microtexture, structure and mechanical properties [J]. Fibre Science Technology, 1986, 27(1): 1-23.

[9] Paris O, Loidl D, Peterlik H. Texture of PAN- and pitch-based carbon fibers [J]. Carbon, 2002, 40(4): 551-555.

[10] Rahaman M S A, Ismail A F, Mustafa A. A review of heat treatment on polyacrylonitrile fiber [J]. Polymer Degradation and Stability, 2007, 92(8): 1421-1432.

[11] Li D H, Lu C X, Wu G P, et al. Structural evolution during the graphitization of polyacrylonitrile-based carbon fiber as revealed by small-angle X-ray scattering [J]. Journal of Applied Crystallography, 2014, 47(6): 1809-18.

[12] Li D H, Lu C X, Du S J, et al. Structural features of various kinds of carbon fibers as determined by small-angle X-ray scattering [J]. Applied Physics A, 2016, 122(11): 956.

[13] Li D H, Lu C X, Wu G P, et al. Heat-induced Internal Strain Relaxation and its Effect on the Microstructure of Polyacrylonitrile-based Carbon Fiber [J]. Journal of Materials Science & Technology, 2014, 30(10): 1051-1058.

[14] Li D H, Lu C X, Wu G P, et al. Structural heterogeneity and its influence on the tensile fracture of PAN – based carbon fibers [J]. RSC Advances, 2014, 4(105): 60648-51.

[15] Griffith A A. The phenomena of rupture and flow in solids [J]. Philosophical Transactions of the Royal Society of London, 1921, 221(1921): 163-198.

[16] Phillips D C. The fracture energy of carbon-fibre reinforced glass [J]. Journal of Materials Science, 1972, 7(10): 1175-1191.

[17] Ruland, W. X-Ray Studies on Preferred orientation in carbon fibers[J]. Journal of Applied Physics, 1967, 38(9): 3585-3589.

[18] Ruland W. Small-angle scattering of two-phase systems: determination and significance of systematic deviations from porod's Law [J]. Journal of Applied Crystallography, 1971, 4(1): 70-73.

[19] Northolt M G, Veldhuizen L H, Jansen H. Tensile deformation of carbon fibers and the relationship with the modulus for shear between the basal planes [J]. Carbon, 1991, 29(8): 1267-1279.

[20] Ruland W. The relationship between preferred orientation and Young's modulus of carbon fibers; proceedings of the Appl Polym Symp, F, 1969 [C]. American Chemical Society.

[21] Fischer L, Ruland W. The influence of graphitization on the mechanical properties of carbon fibers [J]. Colloid and Polymer Science, 1980, 258(8): 917-922.

[22] Li D H, Lu C X, Wang L N, et al. A reconsideration of the relationship between structural features and mechanical properties of carbon fibers [J]. Materials Science and Engineering: A, 2017, 685(2017): 65-70.

[23] Wang D S, Chang S Y, Huang Y C, et al. Nanoscopic observations of stress-induced formation of graphitic nanocrystallites at amorphous carbon surfaces [J]. Carbon, 2014, 74(0): 302-311.

[24] Zaldivar R J, Rellick G S. Some observations on stress graphitization in carbon-carbon composites [J]. Carbon, 1991, 29(8): 1155-1163.

[25] Liu F J, Wang H J, Xue L, et al. Effect of microstructure on the mechanical properties of PAN-based carbon fibers during high-temperature graphitization [J]. Journal of Materials Science, 2008, 43(12): 4316-4322.

[26] Kobayashi T, Sumiya K, Fukuba Y, et al. Structural heterogeneity and stress distribution in carbon fiber monofilament as revealed by synchrotron micro-beam X-ray scattering and micro-Raman spectral measurements [J]. Carbon, 2011, 49(5): 1646-1652.

[27] Kobayashi T, Sumiya K, Fujii Y, et al. Stress concentration in carbon fiber revealed by the quantitative analysis of X-ray crystallite modulus and Raman peak shift evaluated for the variously-treated monofilaments under constant tensile forces [J]. Carbon, 2013, 53(0): 29-37.